

Thermo-mechanical Analysis of Lithium-ion Batteries with Variable Reversible Heat Source

YaohongSuo*, Guanghui Lai, Mingju Lin

School of Mechanical Engineering and Automation, Fuzhou University, Fuzhou, 350108, China

*E-mail: yaohongsuo@126.com

Received: 16 February 2022/ Accepted: 31 May 2022 / Published: 4 July 2022

Capacity fade and mechanical degradation are the main reasons to hinder the development of lithium-ion batteries. Temperature rise and thermal stress can lead to explosion and failure of LIBs during charge or discharge. In this work, in order to understand the mechanism of the temperature rise, the reversible heat source is regarded to be variable with SOC not constant, and a full thermo-mechanical coupling model is developed on basis of the heat transfer equation and mechanical equilibrium equation. Then numerical calculations are simulated to investigate the temperature and stress distributions of 18650 cylindrical LIBs. Simultaneously, the influences of the discharge current, ambient temperature and conductive heat transfer on the temperature, radial and hoop stresses are discussed. Finally, the temperature, radial and hoop stresses are compared in different coupling models and different heat sources, respectively. Numerical results show that the variable reversible heat source is more reasonable, and the discharge current, ambient temperature and the convective heat transfer are sensitive to the temperature, radial and hoop stress distributions. In order to avoid the temperature rise and reduce the magnitude of the stress, one should decrease the discharge current or enhance the conductive heat transfer coefficient.

Keywords: Thermo-mechanical coupling; Variable reversible heat source; Temperature, Radial stress, Hoop stress

1. INTRODUCTION

Lithium-ion batteries (LIBs) are widely used in the electric vehicles and energy storage equipment due to its excellent advantages, such as high voltage, low self-discharge rate, high specific energy and no pollution and so on. However, the bulge, failure and explosions [1] are often reported during charge or discharge owing to thermal runaway. The thermal runaway will result in higher local temperature and the cell expansion which are the main reasons to hinder the rapid development and application of LIBs. Moreover, it can reduce lifetime, cause mechanical degradation and drop the performance of LIBs. Therefore, it is necessary to make clear the mechanism of temperature rise and

expansion, which can provide some references for the design, temperature management and mechanical failure of the battery systems.

More and more attentions are paid to the temperature rise during charge or discharge. For example, Bernardi et al. [2] presented a general energy balance model with reversible and irreversible heat generation rate to estimate the thermal characteristics of the battery. Shadman Rad et al. [3] considered the temperature- and current- dependent overpotential heat generation and state of charge dependent entropy contributions and proposed an adaptive thermal model. Ohshima et al. [4] developed a thermal model to study the temperature rise of small LIBs under discharge process. Mei et al. [5] proposed a thermal model for a pouch cell and analyzed the temperature distribution during discharge. Liu et al. [6] investigated the thermal characterization of LIBs with thermal radiation effect. The thermal abuse is investigated in [7-9], which is benefited for battery systems to evaluate cell thermal behavior. Cheng et al. [10] established a 3D finite element model of battery temperature in a single-layer structure and multi-layer structure. Wang et al. [11] analyzed the effect of structural factors on the heat dissipation in a thermal model. Tian et al. [12] set up a thermo-mechanical coupling model to analyze the thermal stress and total deformation of the battery under fast charging condition. These above researches predict the temperature behavior, but some of them neglect the radiation heat or the influence of the deformation upon the temperature. It is more important that reversible heat source is regarded as constant for the sake of simplicity which does not precisely describe the heat generation during discharge and severely limits the scope of applications.

Another reason leading to fracture and cavitation of LIBs is larger deformation or larger stress. To explore the stress generation induced by temperature rise, some efforts have been committed. Zhao et al. [13] used a coupled lithiation and deformation model to analyze the thermal stress by non-equilibrium thermodynamics. Suo et al. [14] developed a thermo-mechanical coupling model of LIBs to discuss the radial and hoop stress distributions. Xiong et al. [15] analyzed a thermo-mechanical model of external short circuit. Oh et al. [16] investigated the impact of temperature variations on the thermal behaviors of LIBs. Valentin et al. [17] presented the one-way coupling model between temperature and stress to analyze the thermal expansion of the LIBs. Wu et al. [18] presented a multi-physics model of the separator in LIBs, which includes thermo-mechanical-diffusion. Xiao et al. [19] presented a finite element based multi-scale approach for the stress analysis of the separator in a battery cell. The electrochemical-thermal coupling model was developed in [20, 21] omitting the effect of deformation on the temperature. Duan et al. [22] developed a 3D thermal-mechanical model to analyze the von-Mises stress of the LIBs. Mei et al. [23] used a coupled thermal-stress model to describe the thermal expansion behavior of LIBs. In the most of these above coupling studies, the influence of stress on the temperature is not taken into account which is called one-way coupling.

In view of the problems mentioned above, considering the variable reversible heat source, a fully thermo-mechanical coupling model of cylindrical LIBs during discharge is developed in this work. Then taking 18650 LIBs as the object, some numerical simulations are carried out to describe the temperature, radial and hoop stress distributions, and the influences of some parameters upon the temperature, radial and hoop stresses are discussed in the meantime. Finally, some comparisons between the present model and one-way coupling model, between the variable reversible heat source and constant reversible heat source are made.

2. THEORETICAL MODEL OF THERMO-MECHANICAL COUPLING WITH VARIABLE REVERSIBLE HEAT SOURCE

2.1 Heat conduction model

For the sake of simplification, some assumptions [24] of heat conduction are made as follows:

- (1) Heat conduction in the LIBs only occurs along the radial direction;
- (2) The heat conduction rate, density and specific heat capacity are all constants;
- (3) The heat convection appears at the surface of LIBs.

The total amount of heat generation Q [2] includes the heat from internal resistance generation and reversible entropy variable heat from electro-chemical reaction. i.e.,

$$Q = I \cdot (E_{oc} - V_L) - I \cdot T \frac{dE_{oc}}{dT} \quad (1)$$

where Q is the heat generation rate, I is current of discharge, E_{oc} is open-circuit voltage, V_L is voltage, T is temperature, and $\frac{dE_{oc}}{dT}$ is the entropy heat coefficient which is valued as [25]

$$\frac{dE_{oc}}{dT} = \frac{\Delta S}{F} \quad (2)$$

in which ΔS is the entropy change and F is Faraday's constant (=96485 C/mol).

Substituting Eq. (2) into (1) yields

$$q = (I^2 \frac{E_{oc} - V_L}{I} - I \cdot T \frac{\Delta S}{F}) / V = (I^2 R - I \cdot T \frac{\Delta S}{F}) / V \quad (3)$$

where q , R ($= \frac{E_{oc} - V_L}{I}$) and V are the heat generation rate per volume, the electric resistance and the volume of the battery, respectively. According to the work from Inui et al. [26], ΔS is expressed as follows

$$\Delta S = \begin{cases} 99.88\text{SOC} - 76.67 & 0 \leq \text{SOC} \leq 0.77 \\ -30 & 0.77 < \text{SOC} \leq 0.87 \\ -20 & 0.87 < \text{SOC} \leq 1 \end{cases} \quad (4)$$

and SOC [25] is

$$\text{SOC} = 1 - \frac{I \cdot t}{C_0} \quad (5)$$

in which C_0 is battery capacity (=2.2 Ah). It is noted that the reversible heat source is variable depending on the state of charge (SOC) and not constant which is different from those studies carried out previously.

The heat transfer differential equation related to the deformation is given as reported in [27]

$$k \left(\frac{\partial^2 T}{\partial r^2} + \frac{1}{r} \frac{\partial T}{\partial r} \right) + q = \rho C_e \frac{\partial T}{\partial t} + (3\lambda + 2G) \alpha T_0 \frac{\partial \varepsilon_{kk}}{\partial t} \quad (6)$$

where k , t , ρ , C_e , α and T_0 are the thermal conductivity coefficient, time, density, specific heat capacity and thermal expansion coefficient and initial temperature, respectively. ε_{kk} is the volume strain with $\varepsilon_{kk} = \varepsilon_r + \varepsilon_\theta + \varepsilon_z$ in which ε_r , ε_θ and ε_z denote radial, hoop and axial strain, respectively.

$\lambda (= \frac{\nu E}{(1+\nu)(1-2\nu)})$ and $G (= \frac{E}{2(1+\nu)})$ are Lamé constants in which E and ν are Young's modulus and Poisson ratio, respectively. Noticing that Eq. (3) and (6) constitute the heat conduction equation affected by the deformation with variable reversible heat source.

2.2 Mechanical equilibrium equation

Suppose that zero body forces are acting on the cylinder LIBs, the mechanical equilibrium equation requires that

$$\frac{\partial \sigma_r}{\partial r} + \frac{\sigma_r - \sigma_\theta}{r} = 0 \quad (7)$$

where σ_r and σ_θ are the radial stress and the hoop one, respectively.

The relationships of the displacement and the strains are

$$\varepsilon_r = \frac{\partial u}{\partial r}, \quad \varepsilon_\theta = \frac{u}{r} \quad (8)$$

where u is the radial displacement.

According to the linear elastic theory, the stress-strain relationships related to the temperature are written as

$$\begin{aligned} \sigma_r &= 2G\varepsilon_r + \lambda\varepsilon_{kk} - \beta(T - T_f) \\ \sigma_\theta &= 2G\varepsilon_\theta + \lambda\varepsilon_{kk} - \beta(T - T_f) \\ \sigma_z &= \lambda(\varepsilon_r + \varepsilon_\theta) - \beta(T - T_f) \end{aligned} \quad (9)$$

where $\beta (= \frac{\alpha E}{1-2\nu})$ denotes a thermo-mechanical coupling coefficient and T_f the reference temperature.

Combining with Eqs. (7)-(9), the equilibrium equation is expressed in terms of displacement in the following

$$\frac{\partial^2 u}{\partial r^2} + \frac{1}{r} \frac{\partial u}{\partial r} - \frac{u}{r^2} = \alpha \frac{1+\nu}{1-\nu} \frac{\partial T}{\partial r} \quad (10)$$

2.3 Initial and boundary conditions

Suppose the initial temperature of the battery is T_0 and there is no deformation at the initial. This leads to the following initial conditions

$$T(r, t)|_{t=0} = T_0, \quad u(r, t)|_{t=0} = 0 \quad (11)$$

Because of the symmetry of cylinder and boundary condition in the LIBs, the displacement and heat flux N at the center is always zero during the charge or discharge. Additionally, suppose that there is no radial load at the surface [28] and the surface satisfies the Newton cooling formula [17]. i.e., the corresponding boundary conditions are written as

$$u|_{r=0} = 0, \quad \sigma_r|_{r=r_0} = 0 \quad (12)$$

$$N|_{r=0} = 0, \quad N|_{r=r_0} = h(T - T_h)|_{r=r_0} \quad (13)$$

where r_0 , h and T_h are the radius of the battery, coefficient of the convective heat transfer calculated from the heat losses for a battery model and ambient temperature, respectively.

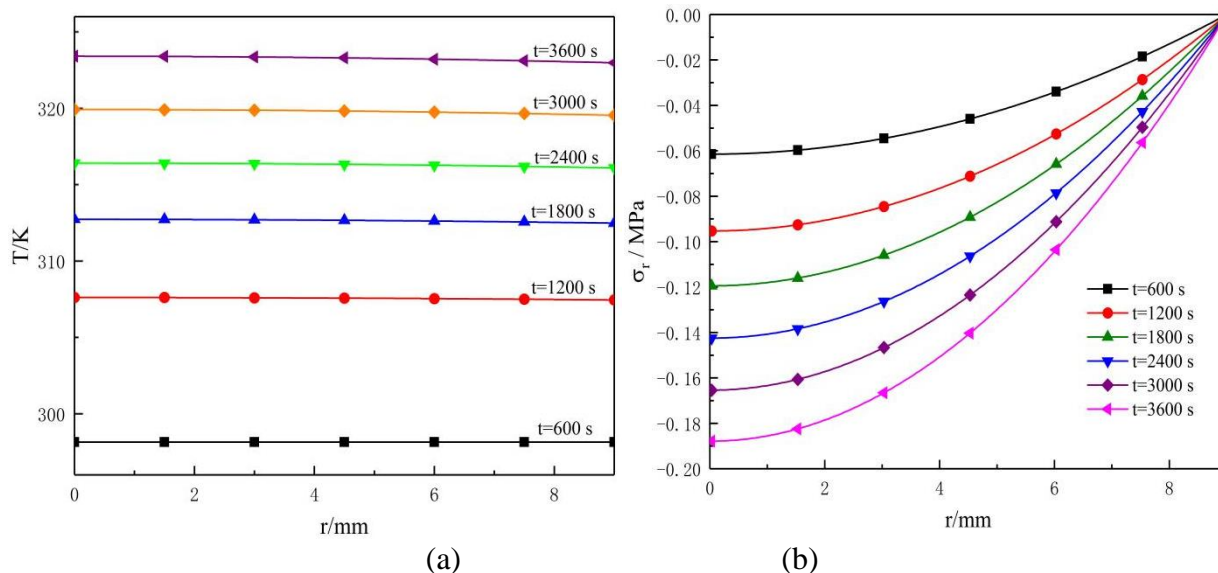
3. NUMERICAL SIMULATION AND DISCUSSION

In order to discuss the influence of variable reversible heat source on the temperature and stress distributions, one takes 18650 LIBs as object to solve Eqs. (6) and (10) with initial and boundary conditions (11)~(13) by COMSOL. Values of some parameters [29] used in the simulation are listed in Table 1.

Table 1. Values of some parameters

Parameters	Symbols	Values
Battery capacity/ Ah	C_0	2.2
Resistance/ Ω	R	0.15
Radius/ mm	r_0	9
Height/ mm	H	65
Initial temperature/ K	T_0	298.15
Density/(kg / m ³)	ρ	2722
Specific heat capacity/(J / (kg · K))	C_e	970
Thermal conductivity coefficient/(W / (m · K))	k	2.6
Young's modulus/ GPa	E	75.42
Poisson ratio	ν	0.325
Thermal expansion coefficient/ K ⁻¹	α	1.38×10^{-5}

3.1 Temperature and stress variations with radius at different discharge times



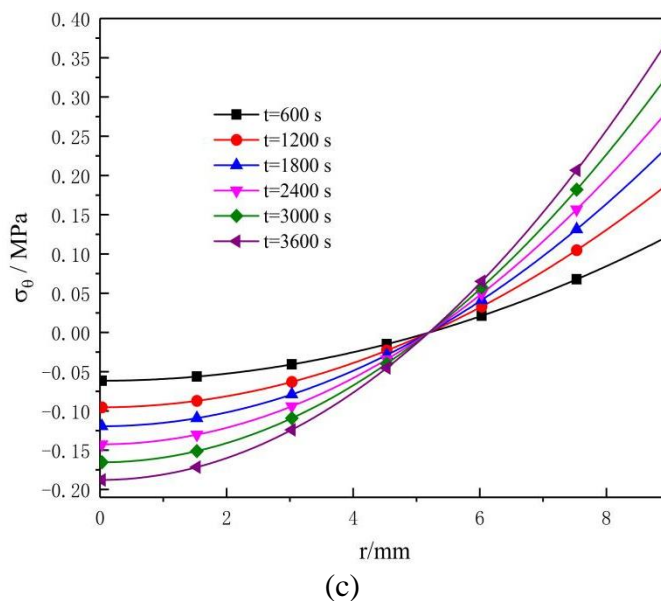


Figure 1. The variations of temperature (a), radial stress (b) and hoop stress (c) with radius at different discharge times for 1 C

Figure 1 depicts the distributions of temperature, radial stress and hoop stress at different discharge times for 1 C and $T_h = 298.15 \text{ K}$, $I = 2.2 \text{ A}$, $h = 10 \text{ W}/(\text{m}^2 \cdot \text{K})$. Seen from Fig. 1(a), the peak of temperature lies at the center at a certain discharge time and it gradually decreases from the center to the surface because the heat dissipation conditions at the surface are better than that at the center owing to the convective heat transfer and heat conduction. However, at a fixed position, the temperature will increase with the increase of the discharge time. Moreover, the temperature at the end of discharge (i.e., $t = 3600 \text{ s}$) at every position will reach the highest among at all the discharge times, and the temperature at the center reaches the peak among the ones at other position at the end of discharge. Thus, in order to ensure the safety of the battery during the discharge, some effective measures should be taken to decrease the temperature.

The distribution of radial stress with different positions is plotted in Fig. 1(b). Obviously the battery undergoes compressive in the radial direction and the compressive stress reaches the peak at the center. At a certain fixed position in the battery, the radial stress is increasing with the increase of the discharge time and it will be the largest at the end of discharge as shown $t = 3600 \text{ s}$. On the other hand, for a same discharge time, the magnitude of the radial stress will reduce from the center to the surface till to zero which satisfies the boundary condition at the surface. The hoop stress versus the radius is demonstrated in Fig. 1(c). As can be seen from this figure that the hoop stress undergoes from the tension near the surface to the compression near the center, and the maximum of hoop stress occurs at the surface which may result in the propagation of surface flaw. Compared with Fig. 1(b) and 1(c), the magnitude of hoop stress is about an order higher than that of radial stress which indicates that temperature rise cause larger hoop expansion. The existed research showed the tensile stress is the main reason leading to the electrode failure [13]. Therefore, the larger tensile hoop stress is more dangerous.

3.2 Some parameters influence on the temperature and stress

In order to quantitatively investigate how the discharge current, ambient temperature and heat convection are sensitive to the temperature, radial and hoop stress, the following numerical calculations are carried out.

(1) The influence of discharge current on the temperature and stress distributions

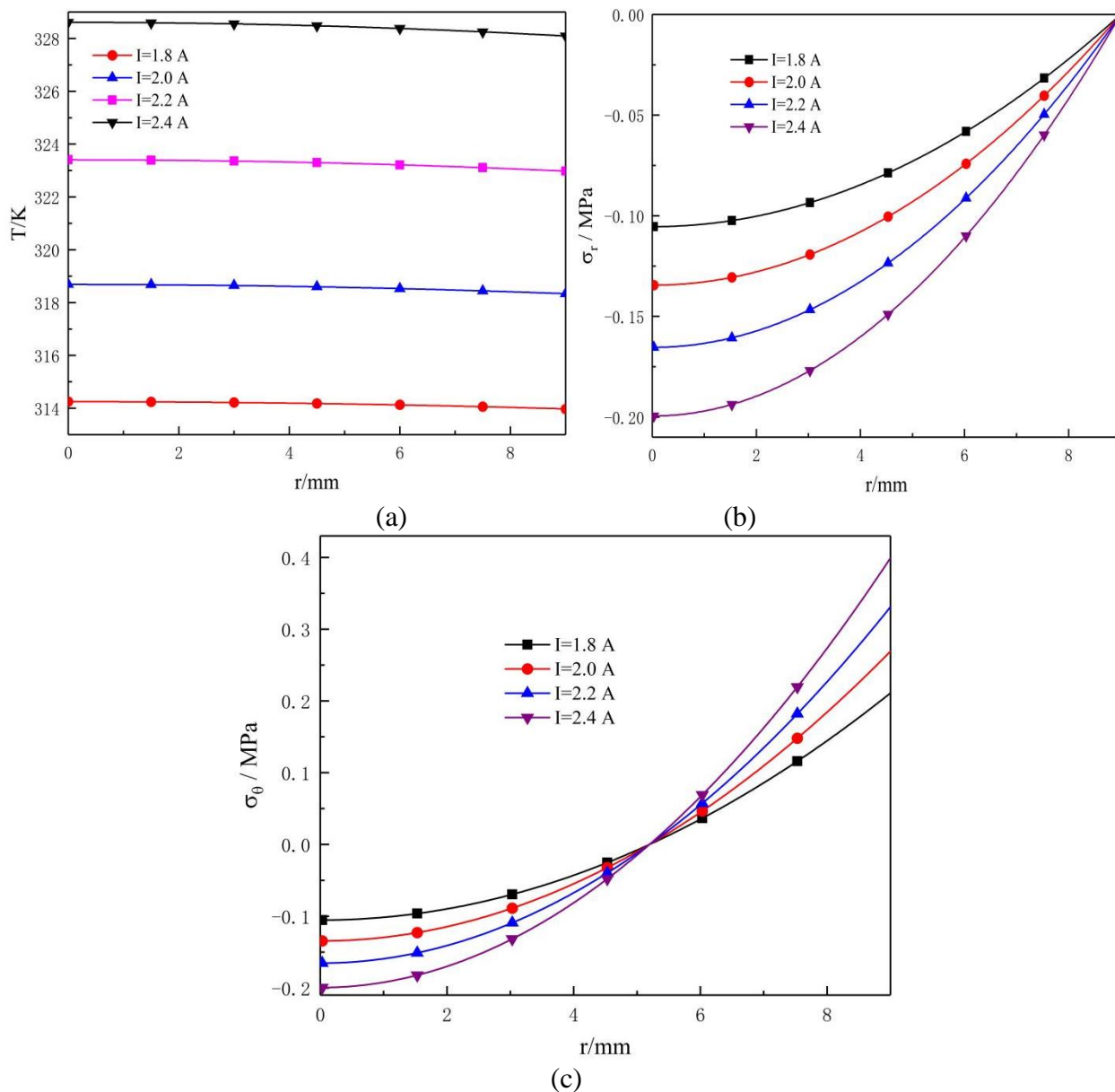


Figure 2. The influence of discharge current on the temperature (a), radial stress (b) and hoop stress (c) for $T_h = 298.15$ K, $h = 10$ W/(m²·K) and $t = 3000$ s

To evaluate the influence of discharge current upon the temperature and stress distributions as shown in Fig. 2 for $T_h = 298.15$ K, $h = 10$ W/(m²·K) and $t = 3000$ s, four different discharge currents are selected to be 1.8 A, 2.0 A, 2.2 A and 2.4 A. Obviously, the temperature, radial stress and

hoop stress all increase when the discharge current increases in Fig. 2(a), 2(b) and 2(c). The reason is due to that higher discharge current results in larger heat generation seen from Eq. (3), and larger heat generation causes the temperature increase, and further bring to larger expansion and larger thermal stress which can be proved from the constitutive equation. In order to avoid the electrode failure or destruction, one should decrease discharge current to reduce the maximum tensile hoop stress.

(2) The influence of ambient temperature on the temperature and stress distributions

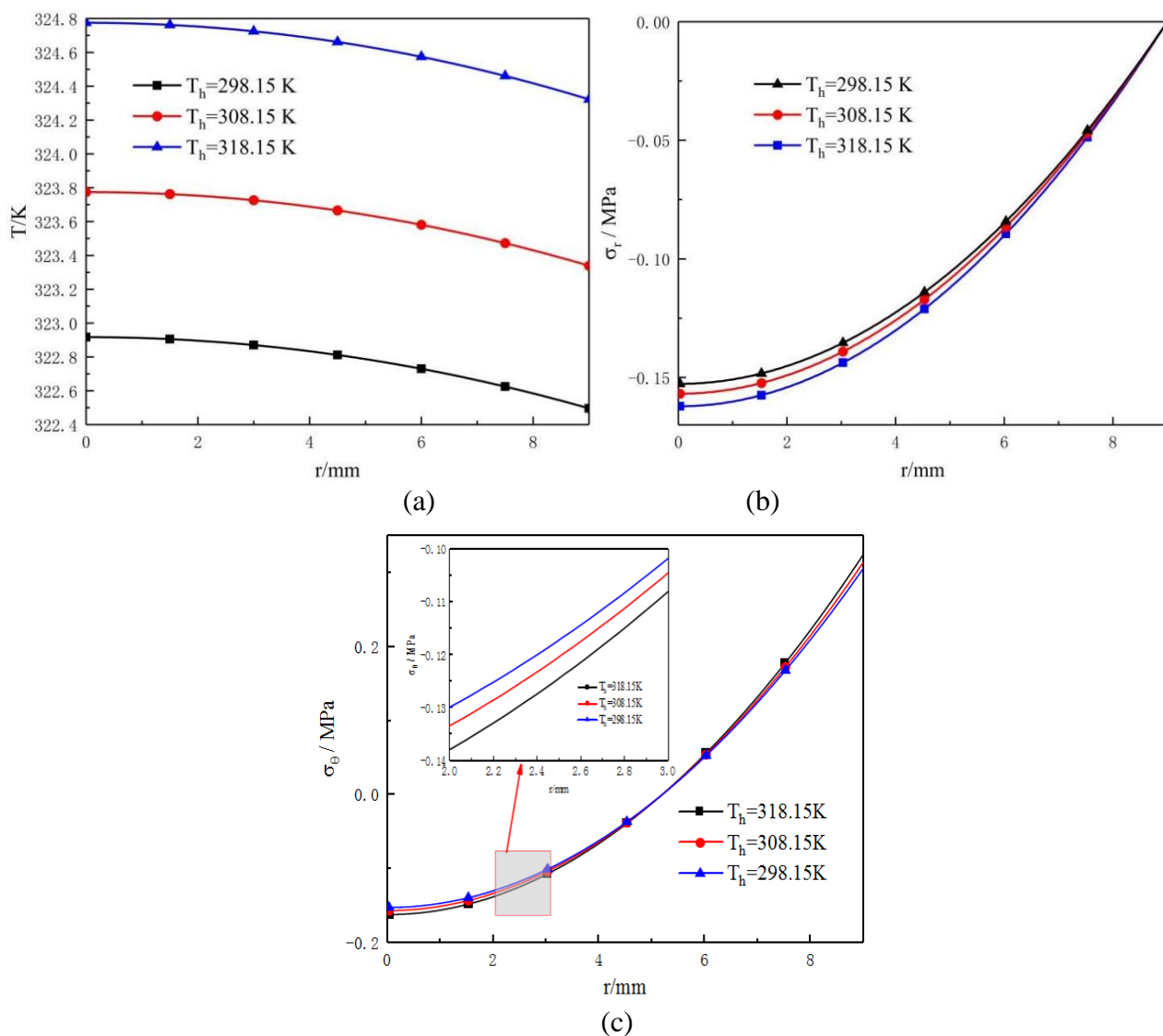


Figure 3. The inference of ambient temperature on the temperature (a), radial stress (b) and hoop stress (c) for $h = 10\text{ W}/(\text{m}^2 \cdot \text{K})$ 、 $I = 2.2\text{ A}$ and $t = 3000\text{ s}$

Figure 3 describes the influence of the ambient temperature on the temperature, radial stress and hoop stress for $h = 10\text{ W}/(\text{m}^2 \cdot \text{K})$, $I = 2.2\text{ A}$ and $t = 3000\text{ s}$. The numerical results reveal that 1) the distributions of the temperature and radial stress is dependent on the ambient temperature while the ambient temperature has little effect on the hoop stress; 2) As the ambient temperature increases, the

temperature of the LIBs also increases and the temperature rise will decrease. Such a trend is consistent with that in [30]; 3) The radial stress and hoop stress reduce as the ambient temperature decreases.

(3) The influence of convective heat transfers on the temperature and stress distributions

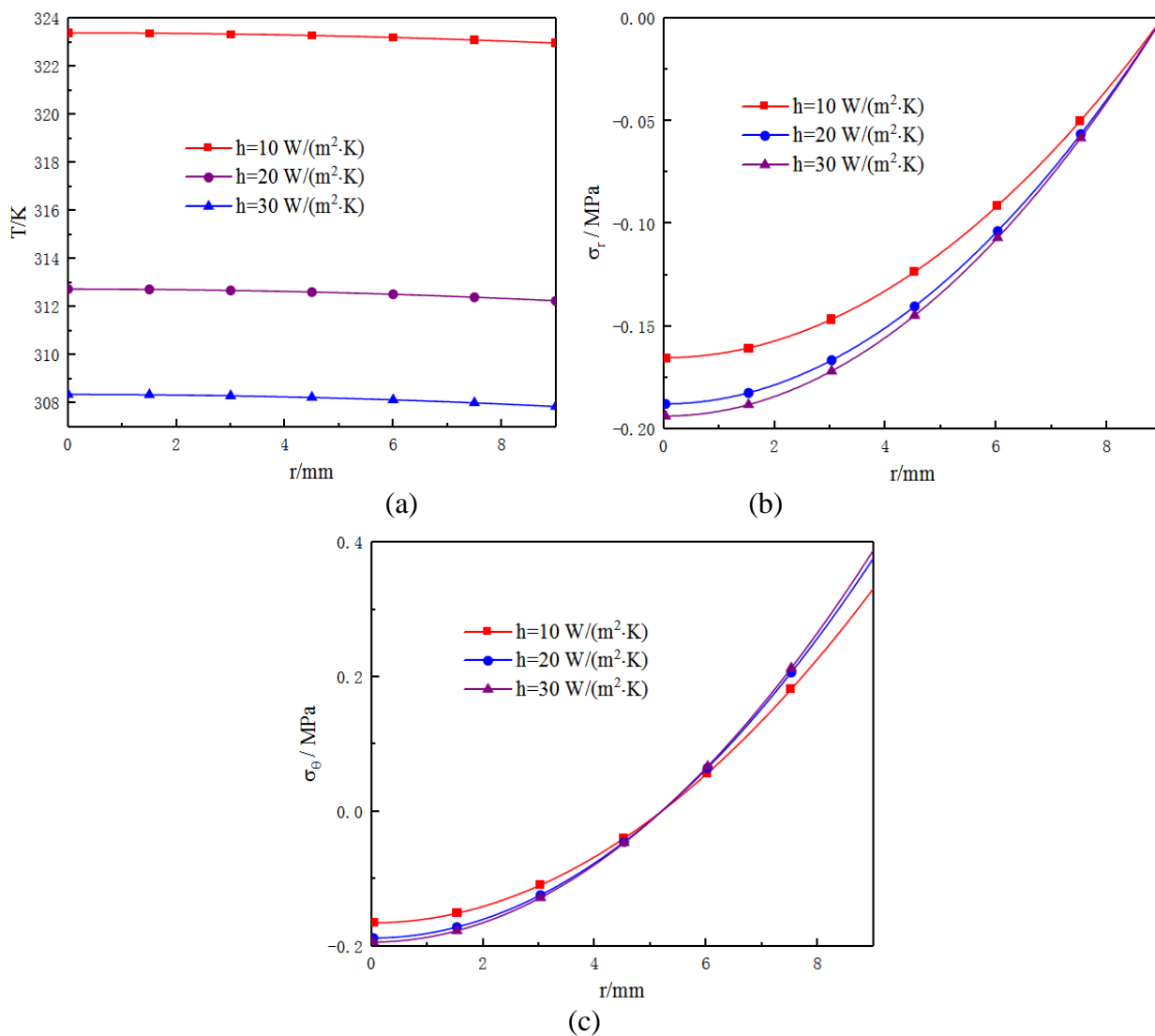


Figure 4. The influence of heat convection on the temperature (a), radial stress (b) and hoop stress (c) for $T_h = 298.15$ K, $I = 2.2$ A and $t = 3000$ s

To disclose the temperature and stress profiles affected by different convective heat transfer, Fig. 4 plots the influence of heat convection on the temperature, radial stress and hoop stress for $T_h = 298.15$ K, $I = 2.2$ A and $t = 3000$ s. It is observed from Fig. 4(a) that the larger the heat convection is, the smaller the temperature of the battery is. This is because the larger heat convection means more heat exchange between the battery and the surround environment which results in lower temperature of

battery. To avoid higher temperature in the battery, one should adopt forced convective not natural convection heat transfer to improve the convective heat transfer.

The convective heat transfer has a pronounced influence on the radial and hoop stresses as shown in Figs. 4(b) and 4(c). It can be seen that when the convective heat transfer coefficient increases, the stress increases gradually at a certain fixed position, while the amplitude of the stress increases smaller when the convective heat transfer coefficient increases to $30 \text{ W}/(\text{m}^2 \cdot \text{K})$. Summing up the influences of the convective heat transfer upon the temperature and stress distributions, a larger convective heat transfer decreases the battery temperature prominently but increases the stress. Therefore, one should choose an electrode material with larger convective heat transfer to decrease the temperature of the battery.

4. COMPARISONS

a) The comparisons of temperature, radial and hoop stress between variable and constant reversible heat source

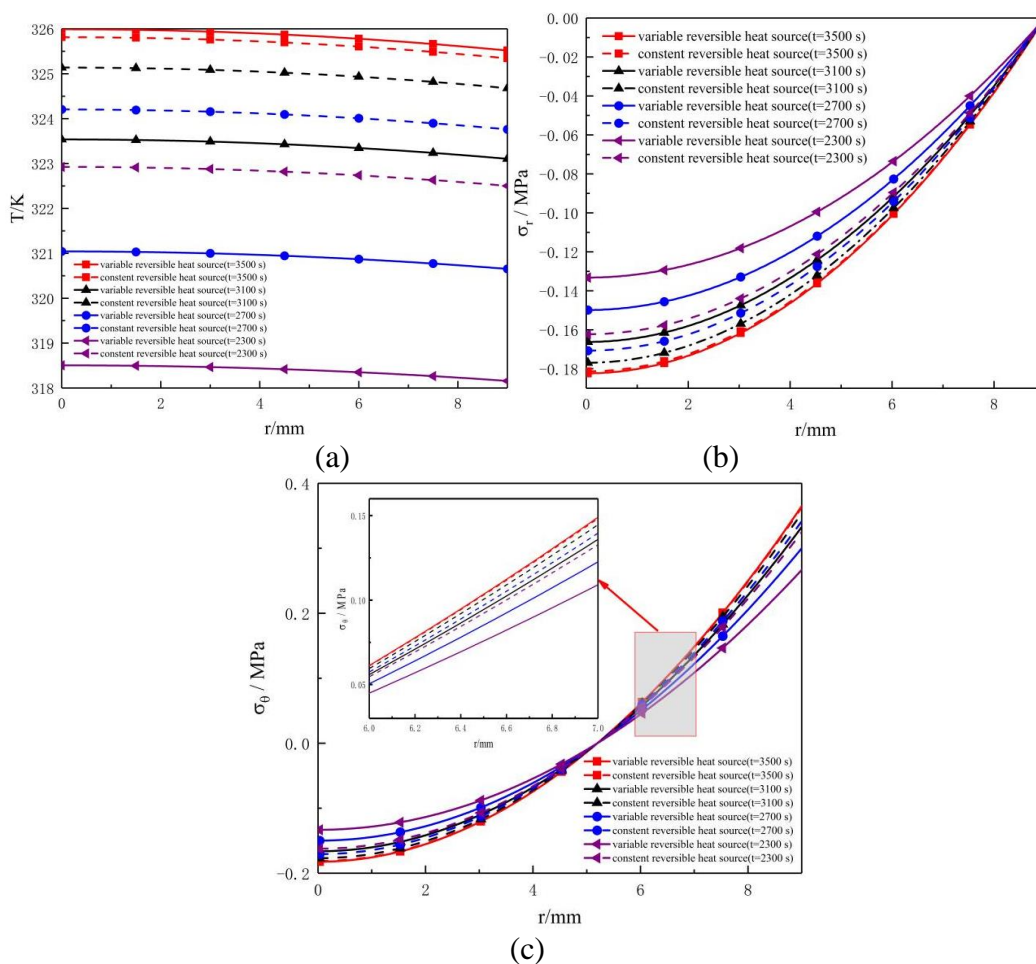


Figure 7. The comparisons of temperature (a), radial stress (b) and hoop stress (c) between the variable and constant reversible heat source

In order to illustrate how much the variable reversible heat source affects the temperature, radial and hoop stress, Fig. 7 compares two cases: variable and constant reversible heat source during the discharge. It can be observed that the temperature, radial and hoop stress with constant reversible heat source are all higher than those with variable reversible heat source at a certain fixed position for arbitrary discharge times. It is because constant reversible heat generates more heat energy accumulated in the battery which leads to higher temperature and larger thermal stress. It is known that the variable reversible heat source depending on SOC represents a more realistic behavior of heat generation during discharge.

b) The comparisons of temperature, radial and hoop stress between present model and one-way coupling model

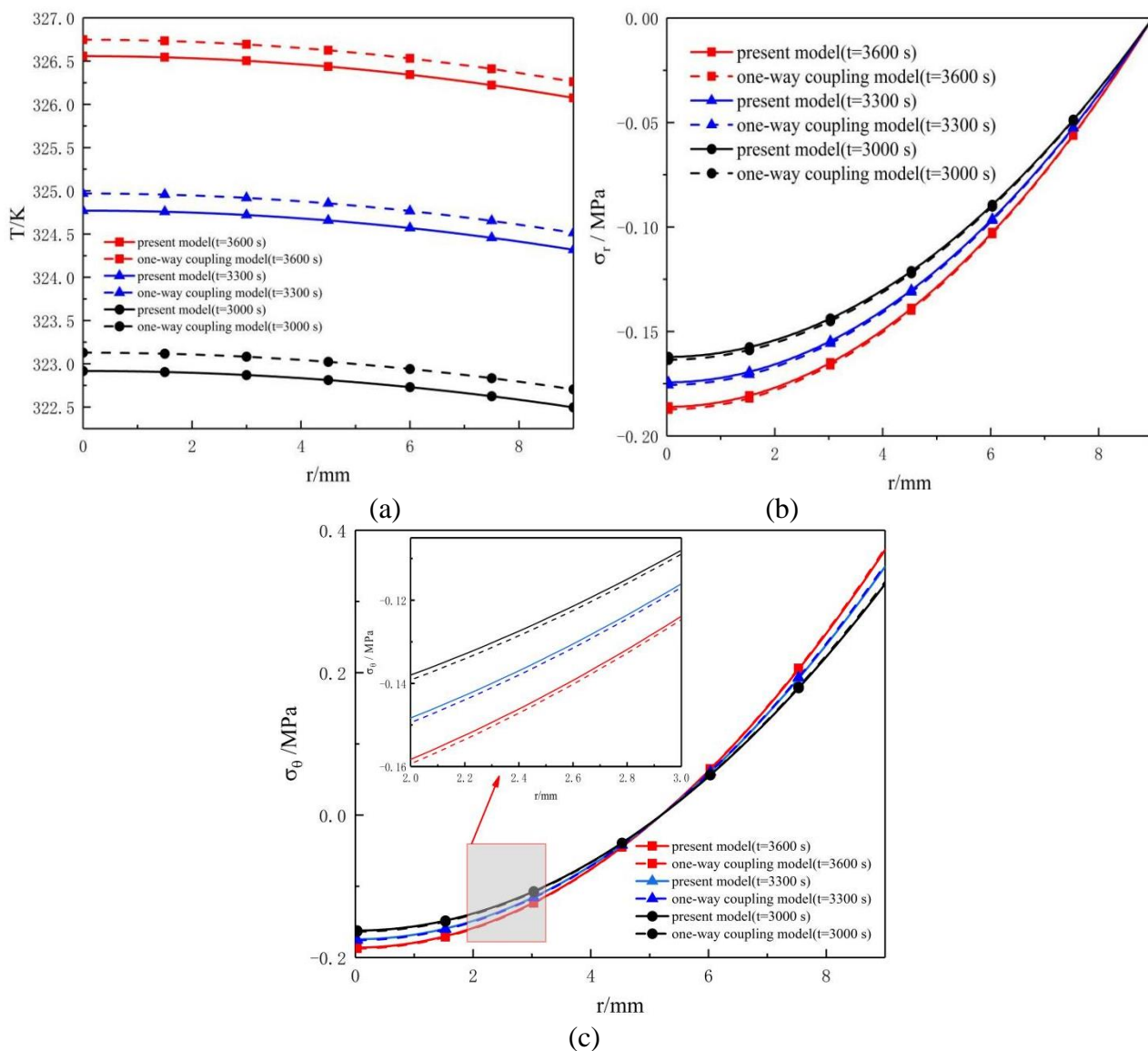


Figure 8. The comparisons of temperature (a), radial stress (b) and hoop stress (c) between present model and one-way coupling model [14]

The comparisons of temperature, radial and hoop stress in the present model and one-way thermo-mechanical coupling model in [14] are performed in Fig. 8(a), 8(b) and 8(c), respectively. One-way thermo-mechanical coupling model is that the thermal equation is pure Fourier heat conduction and mechanical deformation is affected by the temperature. Obviously, one-way coupling model can not characterize the complete thermal behavior due to absence of the deformation effect on the temperature. From 8(a), the variable trends of the temperature are similar in the present model and one-way coupling model. But the temperature of one-way coupling model is higher than that of the present model because some energy from the deformation of the battery is consumed and leads to lower temperature in the present model during the whole discharge. Higher temperature in the one-way model correspondingly results in larger thermal expansion and stress, i.e., higher radial and hoop stress, which can be proved in Fig. 8(b) and 8(c).

5. CONCLUSION

In this work, a fully coupled thermo-mechanical behavior of cylindrical LIBs is investigated with variable reversible heat source. Then taking 18650 LIBs as the object, the temperature and stress distributions are numerically analyzed. Numerical results show that

(1) Higher temperature, larger radial and hoop stresses of the LIBs are observed with the increase of the discharge time. Moreover, the radial stress is always compressive, while the hoop stress near the center is compressive and the hoop stress near the surface is tensile.

(2) The temperature, radial and hoop stress are influenced by the discharge current, ambient temperature and heat convection. It is helpful to decrease the temperature, radial stress and hoop stress when the discharge current and ambient temperature are reduced. However, the temperature of LIBs will be decreased when the heat convection is increased.

(3) The variable reversible heat source is more reasonable and the thermo-mechanical coupling model with constant reversible heat source overestimates the temperature, radial and hoop stresses.

References

1. R. Zhao, S.J. Zhang and J. Liu, *Journal of Power Sources*, 299 (2015) 557-577.
2. D. Bernardi, E. Pawlikowski and J. Newman, *Journal of the Electrochemical Society*, 132(1985) 5-12.
3. M. Shadman Rad, D.L. Danilov, M. Baghalha, M. Kazemeini and P.H.L. Notten, *Electrochimica Acta*, 102(2013) 183-195.
4. T. Ohshima, M. Nakayama, K. Fukuda, T. Araki and K. Onda, *IEEE Transactions on Power and Energy*, 124 (2004) 1521-1527.
5. W.X. Mei, H.D. Chen, J.H. Sun and Q.S. Wang, *Applied Thermal Engineering*, 142 (2018) 148-165.
6. J. Liu, X.M. Liu, W. Jiang and Y.H. Suo, *Chinese Journal of Power Sources*, 44 (2020) 509-513 (in Chinese).
7. X.N. Feng, X.M. He, M.G. Ouyang, L.G. Lu, P. Wu, C. Kulp and S. Prasser, *Applied Energy*, 154 (2015) 74-91.
8. P. Ping, Q.S. Wang, Y.M. Chung and J. Wan, *Applied Energy*, 205 (2017) 1327-1344.

9. D.P. Kong, G.Q. Wang, P. Ping and J. Wen, *Applied Thermal Engineering*, 189 (2021) 116661.
10. H.Z. Cheng, L.J. Zhang, C. Ruan and K. Diao, *Journal of Tongji University*, 41 (2013) 1249-1254 (in Chinese).
11. Z.P. Wang, W.T. Fan and P. Liu, *Energy Procedia*, 105 (2017) 3339-3344.
12. S. Tian and J.J. Xiao, *Science Technology and Engineering*, 21 (2021) 2725-2729 (in Chinese).
13. K.J. Zhao, M. Pharr, S.Q. Cai, J.J. Vlassak and Z.G. Suo, *Journal of the American Ceramic Society*, 94 (2011) S226-S235.
14. Y.H. Suo and J. Liu, *International Journal of Energy Research*, 45 (2020) 1988-1998.
15. R. Xiong, S.X. Ma, R.X. Yang and Z.Y. Chen, *Journal of Mechanical Engineering*, 55 (2019) 115-125 (in Chinese).
16. K.Y. Oh and B.I. Epureanu, *Applied Energy*, 178 (2016) 633-646.
17. O. Valentin, P.X. Thivel, T. Kareemulla, F. Cadiou and Y. Bultel, *Journal of Energy Storage*, 13 (2017) 184-192.
18. W. Wu, X.R. Xiao, X.S. Huang and S. Yan, *Computational Materials Science*, 83 (2014) 127-136.
19. X.R. Xiao, W. Wu and X.S. Huang, *Journal of Power Sources*, 195 (2010) 7649-7660.
20. F. Bahiraei, M. Ghalkhani, A. Fartaj and G.A. Nazri, *Applied Thermal Engineering*, 125 (2017) 904-918.
21. A. Greco and X. Jiang, *Journal of Power Sources*, 315 (2016) 127-139.
22. X.T. Duan, W.J. Jiang, Y.L. Zou, W.X. Lei and Z.S. Ma, *Journal of Materials Science*, 53 (2018) 10987-11001.
23. W.X. Mei, Q.L. Duan, W. Lu, J.H. Sun and Q.S. Wang, *Journal of Cleaner Production*, 274 (2020) 122643.
24. S.C. Chen, C.C. Wan and Y.Y. Wang, *Journal of Power Sources*, 140 (2005) 111-124.
25. H. Fathabadi, *Journal of Power Sources*, 245 (2014) 495-500.
26. Y. Inui, Y. Kobayashi, Y. Watanabe, Y. Watase and Y. Kitamura, *Energy Conversion and Management*, 48(2007) 2103-2109.
27. C. Zhang, Z. Xu and S. Liu, *Journal of Xi'an Jiaotong University*, 48(2014) 68-72 (in Chinese).
28. H. Hu, P.F. Yu and Y.H. Suo, *Acta Mechanica*, 231 (2020) 2669-2678.
29. J. Dong Hyup and B. Seung Man, *Energy Conversion & Management*, 52 (2011) 2973-2981.
30. L.M. Wang, J.Y. Niu, W. Zhao, G.C. Li and X.L. Zhao, *International Journal of Energy Research*, 43 (2019) 2086-2107.